American Journal of Pathology, Vol. 129, No. 2, November 1987

A Morphometric Study of Reye's Syndrome

Correlation of Reduced Mitochondrial Numbers and Increased Mitochondrial Size With Clinical Manifestations

CYNTHIA C. DAUGHERTY, MD, PETER S. GARTSIDE, PhD, JAMES E. HEUBI, MD, KATHLEEN SAALFELD, and JEAN SNYDER

From the Divisions of Pathology and Gastroenterology, Children's Hospital Medical Center, Departments of Pediatrics and Environmental Health, University of Cincinnati, Cincinnati, Ohio

Morphometric analysis of liver ultrastructure in 14 children with Reye's syndrome (RS) of varying morphologic severity was compared with that of 6 children with normal livers. Results showed reduced numbers of enlarged mitochondria in RS. Multivariant analysis identified correlations between increased mitochondrial size, decreased mitochondrial number, and severity of neurologic disease (stage). A disproportionate increase in mitochondrial area and perimeter in the RS cases with the most depressed mitochondrial number distinguished the 4 children with residual neurologic damage or death. Serum salicylate concentrations were negatively correlated with severity of morphologic alteration. Two cases of non-RS salicylate toxicity showed normal or near-normal mitochondrial size and number. In fatty liver from an autopsy specimen from a child, a child with carnitine deficiency, and a child on therapy for dermatomyositis, mitochondrial numbers were also normal. Decreased mitochondrial numbers are characteristic of RS and imply a pathophysiologic mechanism, possibly related to impaired mitochondrial replication. Synergism with other forms of mitochondrial injury, such as salicylates, hypoglycemia, or shock may influence clinical severity, progression, and outcome. (Am J Pathol 1987, 129:313–326)

THE EVIDENCE that Reye's syndrome (RS)[1] is due to mitochondrial malfunction is compelling.[2] Ultrastructural examination of biopsy liver from children with RS reveals structural alteration of mitochondria.[3] Enzyme histochemical studies on these biopsies reveal decreased staining for enzyme activity localized to mitochondria, with normal intensity of reaction for other enzymes.[4] Biochemical analysis of livers of children with RS has usually demonstrated a reduced level of only those enzymes localized to mitochondria.[2,5] However, deficiencies of known mitochondrial functions do not provide an adequate explanation for all aspects of the disease.[6] The relationship between liver malfunction and the manifestations of central nervous system disease, for example, remains obscure. Although the liver lesion is impressive and accessible to direct investigation in biopsy samples, central nervous system effects of the disease, routinely accessible only through clinical stage, are responsible for its morbidity and mortality. Mitochondrial ultrastructural alterations similar to those in RS liver have been described in neurons in a limited number of cases[7]; however, mitochondrial enzymes in brain and muscle from patients with RS are preserved as compared with liver.[8] Factor analysis, a statistical tool for the analysis of bivariate correlations between variables, implies a disassociation between hepatic impairment as measured by transaminases and encephalopathic features as measured by admission coma stage and ammonia.[9] The liver alteration is thus an imperfect mirror of the process in the brain, and it remains unknown whether the central nervous system is responding to a toxic stimulus in parallel to that affecting the liver or whether the brain injury is mediated by the liver injury.

Supported by a grant from the trustees of Children's Hospital Research Foundation.

Accepted for publication June 22, 1987.

Address reprint requests to Cynthia C. Daugherty, MD, Assistant Professor Pathology and Pediatrics, Children's Hospital Medical Center, Elland and Bethesda Avenues, Cincinnati, OH 45229.

Specificity of the clinical and pathologic manifestations of RS is also sometimes questioned.[10,11] Clinical symptoms of RS overlap with those of various toxic and metabolic disorders. Routine hematoxylin and eosin (H&E)-stained paraffin block sections are not interpretable as specific for RS. Lipid is not specific, accumulating in liver, heart, and renal tubules in many diverse situations related to severe illness.[12] Only the characteristic mitochondrial alterations clearly distinguish RS from other clinically similar diseases. However, demonstration of the mitochondrial lesion by enzyme histochemistry is difficult to control and interpret when not routinely performed. The mitochondrial alteration as demonstrated by ultrastructure is easily obscured by superimposed shock induced swelling, postmortem autolysis, and hypotonic fixation.

Despite these difficulties, subjective assessment of the severity of hepatic alteration has been shown to correlate, at least to some extent, with severity of clinical illness.[13-15] This study sought to define individual quantifiable aspects of the subjectively perceived lesion and to correlate these one with another, as well as with selected laboratory and clinical features. Data were analyzed for specificity and features or combinations of features which might help to explain the pathophysiology, in particular the central nervous system manifestations, of RS.

Materials and Methods

Cases and controls (Table 1) were identified from file cases biopsied between 1973 and 1985 on the basis of 1) the availability of oriented sections with a balanced representation of all portions of the lobule and 2) the severity of ultrastructural alteration, to include the entire range of morphologic change. The mitochondrial alterations required for the diagnosis of RS include enlargement, shape irregularity, increased electron lucency of the matrix, and diminished numbers or absence of matrix granules. Other alterations include lipid accumulation, glycogen depletion, proliferation of smooth endoplasmic reticulum, and peroxisomal flocculent swelling. More advanced changes include endoplasmic reticulum vesiculation, ribosomal disaggregation, and membrane fragmentation of various organelles.[3,4] The 14 RS cases thus selected were grouped by severity on the basis of the following previously published qualitative criteria: Cases showing only regional mitochondrial alteration without changes in other organelle systems were classified as mild (Grade 1). Cases in which all mitochondria are abnormal but with areas in which not all four of the mitochondrial features are present and with mild to moderate changes in other organelles, were classified as moderate (Grade 2). In Grade 3 cases (severe) all areas examined show all four mitochondrial features with variably severe, sometimes advanced, changes in other organelles.[14] One case was assigned Grade 4 because of a narrow midzonal band of hepatocellular necrosis, although elsewhere the lesion resembles Grade 3. The characteristic ultrastructure of each group is illustrated in Figure 1. The 6 morphologically normal controls (Grade 0) comprise 2 children biopsied for biochemical analysis of the enzyme abnormality in phenylketonuria (PKU) (patients JD and HO), 2 unaffected siblings of a child with Wilson's disease (patients WC and JC), and 2 RS patients who had biopsies following recovery (patients RB and JN), follow-up biopsies having been obtained before it was understood that children recovered without hepatic sequelae. Five disease controls include 2 children with toxic salicylate levels (patients SB and MS) and 3 patients with fatty liver for non-RS-related reasons (patients IC, EC, and TD). Tissue from the autopsy liver of IC, the only postmortem sample, was collected within 5 hours of death. Six patients (MS, SB, LH, KK, JC, and KC) were included in previously published reports.[14,16]

Liver biopsies were all performed for appropriate clinical indications to establish a diagnosis. During 1980–1985 minimal criteria for biopsy of children with suspected mild RS were as follows: three times normal SGOT and SGPT in the presence of a resolved or resolving prodromal viral illness, followed by vomiting, with or without clinical manifestations of encephalopathy (lethargy and/or coma). Encephalopathy was staged by previously described criteria.[17] Routine histologic studies on all cases confirmed the diagnosis and ruled out alternate disease. Results of the last blood sample prior to biopsy were analyzed. Laboratory values are in standard units except for prothrombin time, calculated by subtracting the patient's from the control level. All prothrombin times less than 0 were entered as 0.

Liver biopsy samples were usually obtained within five hours of admission. Tissue was collected at the bedside and subdivided for light-microscopic, ultrastructural, and frozen-section examination. Electron microscopy (Philips 400) was performed on tissue fixed in 3% glutaraldehyde in Millonig's buffer, postfixed in 1% osmium tetroxide, and processed into either Epon 812 (c) or LX-112 (c), an Epon equivalent formulated by Ladd after Epon became no longer available. This substitution resulted in no detectable differences in the quality of embedded material and no time- or embedment-related trends are apparent in the data.

Table 1—Case Histories (In Order Studied)

	RB RS	RB Rec	JN RS	JN Rec	JB RS	LH RS	KK RS	JD MNC	NC RS	AR RS	HO MNC	MB RS	WC MNC	JC MNC	JC RS	KC RS	AD RS	KD RS	AE RS	JM RS	MS STC	SB STC	IC FLC	EC FLC	TD FLC
Age years	10.9		11.3		4.3	9.1	12.1	.83	6.2	3.3	10.9	5.0	10.0	4.3	.92	16.3	13.9	5.3	8.9	15.3	4.2	3.3	0	1.4	12.8
Sex	F		M		F	F	F	M	F	F	M	F	M	M	M	F	M	F	F	M	M	F	M	M	F
Prodrome	URI FU		URI FU		URI	VAR	URI	PKU	URI	URI	PKU	URI	ROW	ROW	URI	URI	URI	VAR	URI	URI	SAL TOX	SAL TOX	CHD	CAR	DM
Stage 1 (initial)	4 0		2 0		2	3	1	0	3	3	0	2	0	0	2	1	1	1	3	4	0	0			
Stage 2 (peak)	4		4		4	3	1	0	4	3	0	4	0	0	2	1	1	1	5	5	0	0			
VBI hours	81		100		30	48	40		30	72		38			60	30	36	96	30	40		76			
Sal mg/dl	10.0		1.8		8.6	35.2	19.9		.7	30.3		4.1			17.1	19.3	23.6	2.0		12.2	34.7	29.0			
NH_3 mg/dl			134 28		403	273	123		325	178		375			196	8.4	25.6	36.4	375	540					
SGOT IU	362 13		1280 56		156	562	$^{2}8_{8}2$		424	274		$^{1}3_{5}3$	28	47	246	672	174	$^{1}0_{8}6$	262	$^{1}1_{4}6$	$^{1}5_{4}2$	70			
SGPT IU	416 11		253 48	8	352	744	$^{1}2_{7}0$		583	224		$^{1}0_{4}5$	9	12	150	638	161	$^{1}0_{6}2$	204	892	$^{1}1_{6}6$	50			
PT			3.0		5.8	4.8	0			0.8		5.0			1.2	2.1	1.9	0	.8	3.9	1.5				
Grade	2	2			3	2	1	0	3	1	0	3	0	0	1	1	2	3	3	4	1	1			
Course days	8				11	4	2		8	4		>30			4	2	3	1	13	10	1				
Outcome	W	W			W[1]	W	W		TR[2]	W		R[3]			W	W	W[4]	W	R[5]	D[6]	JRA	W[7]	8	9	10

RS, Reye's syndrome cases; Rec, RS recovery controls; MNC, morphologically normal controls; STC, salicylate toxicity controls; FLC, fatty liver controls; FU, follow-up (RB, 9 weeks; JN, 3 weeks later); URI, upper respiratory tract infection; VAR, varicella infection; PKU, phenylketonuria; ROW, rule out Wilson's disease; SAL TOX, salicylate toxicity; CHD, congenital heart disease; CAR, carnitine deficiency; DM, dermatomyositis; VBI, vomiting biopsy interval; Sal, serum salicylate level; PT, corrected prothrombin time (control seconds subtracted from patient seconds); W, well at discharge, no sequelae; TR, transient residual neurologic symptoms, well at 1-month follow-up; R, residual neurologic symptoms persistent at 1 month or longer; D, death; JRA, juvenile rheumatoid arthritis; CAR, carnitine deficiency; DM, dermatomyositis; /, denotes data not available.

1. Required an intracranial pressure (ICP) monitor.
2. ICP monitor, discharged with ankle clonus and postural instability.
3. ICP monitor, permanent moderate to severe mental retardation.
4. Well at discharge, no further follow-up.
5. ICP monitor, difficulty in school, deep tendon reflexes remained unequal at 1 year.
6. ICP monitor, brain death related to a rapid, uncontrollable rise in intracranial pressure, liver normal at autopsy 10 days later.
7. Presentation with encephalopathy similar to RS, peak serum salicylate 66 mg/dl, decreased to indicated level with hydration by the time of biopsy.
8. Two-day-old with trisomy 21, dysplastic tricuspid valve, and pulmonary stenosis.
9. Recurrent episodes of vomiting and acidosis due to carnitine deficiency.
10. On treatment for dermatomyositis with serum SGOT values ranging from 200 to 300 IU.

Sections from 70 to 80 nm in thickness were photographed at a uniform magnification in an unbiased fashion (upper left or center of all complete grid squares). The electron microscope was calibrated and stable at the magnification used for analysis. Photomicrographs magnified 7200× were measured with a Zeiss Videoplan. All values are reported in micron units. All illustrations were prepared from actually measured electron micrographs.

Standard morphometric techniques[18–23] were adapted to the operational requirements of the Videoplan.[24] The nucleus, nucleolus, and cytoplasmic organelles each were considered as a separate "compartment" nested within the larger compartment of the hepatocyte. Terms are defined and illustrated in Figure 2.

The area (a) and perimeter (p) (circumference) of each profile were measured. The test area (TA) and sums of all areas (A) and perimeters (P) are used by the stereologic programs of the Zeiss Videoplan for calcu-

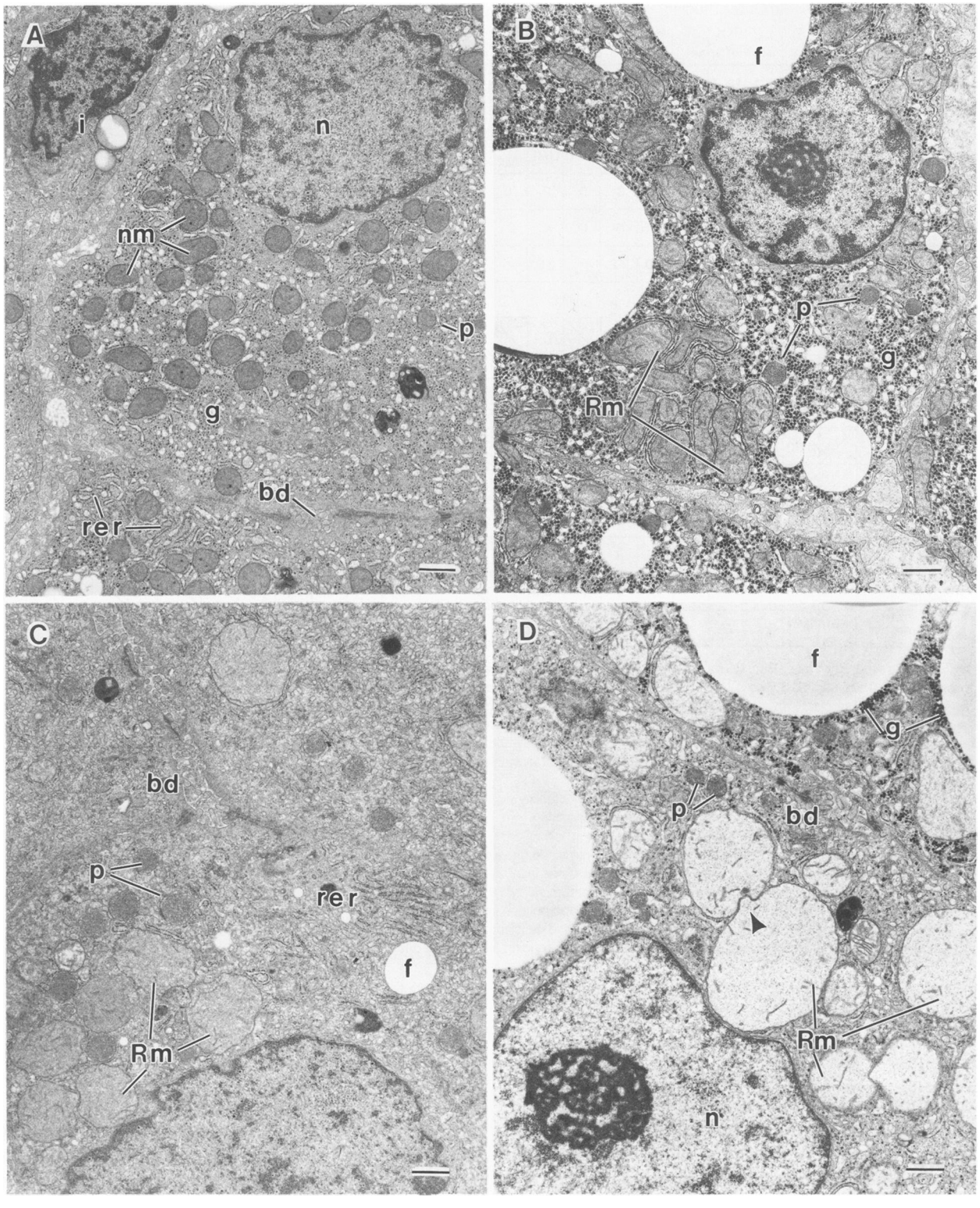

Figure 1—Morphologic range. **A**—Grade 0 (normal) liver (patient JC). **B**—Grade 1 (mild) Reye's syndrome (patient JC). **C**—Grade 2 (moderate) Reye's syndrome (patient AD). **D**—Grade 3 (severe) Reye's syndrome (patient MB). *n*, nucleus; *bd*, bile duct; *i*, Ito cell; *nm*, normal mitochondria; *Rm*, RS mitochondria; *p*, peroxisome; *g*, glycogen; *f*, lipid; *rer*, rough endoplasmic reticulum. *Arrow* indicates apposed membranes (? fusion). Bar = 1 μ.

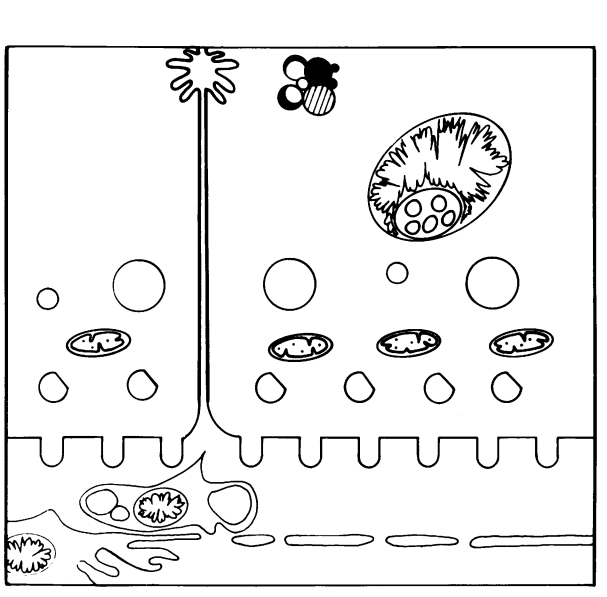

COMPARTMENTS

Residual Bodies (RB)

Nucleus (N)

Nucleolus (No)

Lipid (L)

Mitochondria

Peroxisomes (P)

Hepatocyte (H)

Corrected Test Area (T)

Test Area (TA)

NON MITOCHONDRIAL PARAMETERS

A-Total (sum) Area, prefixed by compartment initial *

TA-Test Area = Total Area of All Pictures

T - Corrected Test Area = HA-LA

a-Mean Profile Area, prefixed by compartment initial *

VV - Volume Density

HVV = (HA-LA)/TA

LVV = LA/HA

all others = *A/T

MITOCHONDRIAL PARAMETERS

NA-Number Per Unit Test Area

a-Mean Profile Area

p-Mean Profile Perimeter

A-Total (sum) Area of Mitochondria

P-Total (sum) Perimeter

N-Total Number of Mitochondria

NV-Numerical Density = $\frac{2}{3\pi}\left(\frac{N \times P}{T \times A}\right)$

SV- Surface Density = $\frac{4}{\pi}\left(\frac{P}{T}\right)$

(a measure of the amount of surface area per unit hepatocyte volume)

S/V-Specific Surface = $\frac{4}{\pi}\left(\frac{P}{A}\right)$

(a measure of the amount of surface area per unit mitochondrial volume)

Figure 2—Study format and formulas. Nonmitochondrial values are prefixed by the compartment initial. When without a prefix, the value under discussion is mitochondrial.

lation of the three dimensional estimates of volume density (VV—total organelle compartment volume per unit test volume), surface density (SV—total organelle surface area per unit test volume), specific surface (S/V—total organelle surface area per unit organelle volume), and numerical density (NV—number per unit test volume). The test area, except as otherwise indicated, was corrected by subtraction of total lipid area (LA) because the greatly increased lipid content of the RS hepatocytes resulted in misleadingly low values of the following calculated parameters: volume density (VV), surface density (SV), and number per unit reference area (NA) or volume (numerical density—NV).

The formulas developed by Zeiss for the stereologic program are derived from several sources as outlined by Underwood.[25] These formulas assume a uniformly sized population of structures of uniform spherical to ovoid shape. The experimental (RS) mitochondria differ from this ideal to a different degree than the controls, thus some bias cannot be excluded. To test the effects of slightly different assumptions, mean tangent diameters were calculated by the method of DeHoff and Rhines[20] and Fullman.[19] The numerical volume was recalculated by the methods of DeHoff and Rhines[17,18] and of Weibel and Gomez.[17,18] The recalculated values approximated or were identical to those generated by the Videoplan.

Because of intralobular variation in lesion severity, measurements from an entire lobule (panlobular) were considered essential for results representative of the functional deficit in the liver. Two studies were limited to the minimum four pictures needed to span a small lobule. The remaining 23 included 5–30 pictures. Two studies (RB—illness and recovery biopsy) had sufficient embedded material to allow for independent analysis of each lobular region. A photomicrograph of each center grid square was used to reconstruct the entire section. The centrilobular zone was defined as the first three to four cell rows adjacent to a central venule, periportal as the first three to four cell rows adjacent to a portal triad, and midzonal as those

cells more than three to four cells from both a central venule and a portal triad. Two blocks, each of which spanned an entire lobule, were analyzed for each zone independently in both the illness and recovery biopsy specimens from patient RB.

Multivariant analysis was performed of the values generated from the 14 RS cases and 6 controls plus the 2 cases of salicylate toxicity. The three non-RS fatty livers were not included in the statistical analysis and are used for comparison. Pearson product-moment correlation coefficients among the several measured parameters of these 22 studies were calculated with the use of the SAS package (SAS Inc.) of computer programs. In the text of this report, negative correlations are emphasized by a minus sign prior to the probability value. Multiple associations were further investigated by scattergram. Comparison among lobular regions and between the disease and recovery liver of RB were initially made by two-way analysis of variance. Specific comparisons were calculated among lobular regions by Scheffe *t* tests. A probability value of less than 0.05 was considered statistically significant, although values greater than 0.01 are not emphasized.

Ultrastructural assessment of cytochrome oxidase activity was performed by the DAB polymerization technique[26] modified to rescue cryoprotected tissue saved frozen at −70 F. The incubations were performed on cryostat frozen sections followed by fixation and embedding in inverted BEEM (c) capsules, which, after polymerization, were used to "pop" the section off the slide.[27] Patients JN and HO were studied.

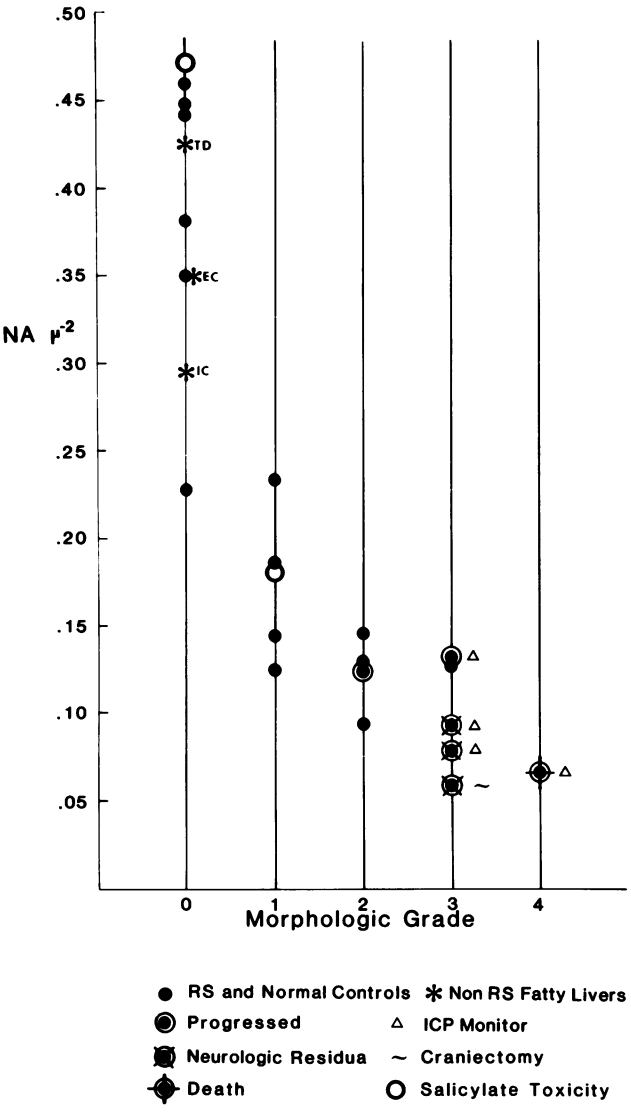

Figure 3—Scattergram. Grade versus mitochondrial number per unit test area (NA). $r = -0.8377$; $P = 0.0001$.

Results

Normal Controls and Comparison With RS Cases

All controls conform qualitatively to established concepts of normal liver. One of the 2 phenylketonuria (PKU) cases tends in terms of mitochondrial number (NA), area (a), and perimeter (p) toward the cases of mild RS (Figures 3 and 4). Periportal hepatocytes in this case contain mitochondria with matrix crystalline arrays. There are no quantitative differences between the two recovery samples (patients JN and RB) and the other normal controls.

A comparison between changes in one child (patient RB) during RS and after recovery illustrates the quantitative alterations observed in RS (Table 2—panlobular comparison). Hepatocytes are greatly distended by lipid in RS. When total lipid is subtracted, the difference between mean hepatocyte area (Ha) in the RS and recovery sample is not significant. Of the nonmitochondrial parameters, the volume densities of lipid (LVV, $P = 0.0001$), residual bodies (RBVV, $P = 0.0011$), and peroxisomes (PVV, $P = 0.0005$), as well as peroxisomal mean area (Pa, $P = 0.0001$) are significantly different on panlobular analysis. RS mitochondria differ from normal mitochondria in two major ways: RS mitochondria are larger and reduced in numbers. The increased size is measurable as a larger area (a, $P = 0.0001$), and perimeter (p, $P = 0.0001$). The reduced numbers (NV, $P = 0.0001$) are reflected in lower volume density (VV, $P = 0.0010$) and surface density (SV, $P = 0.0001$).

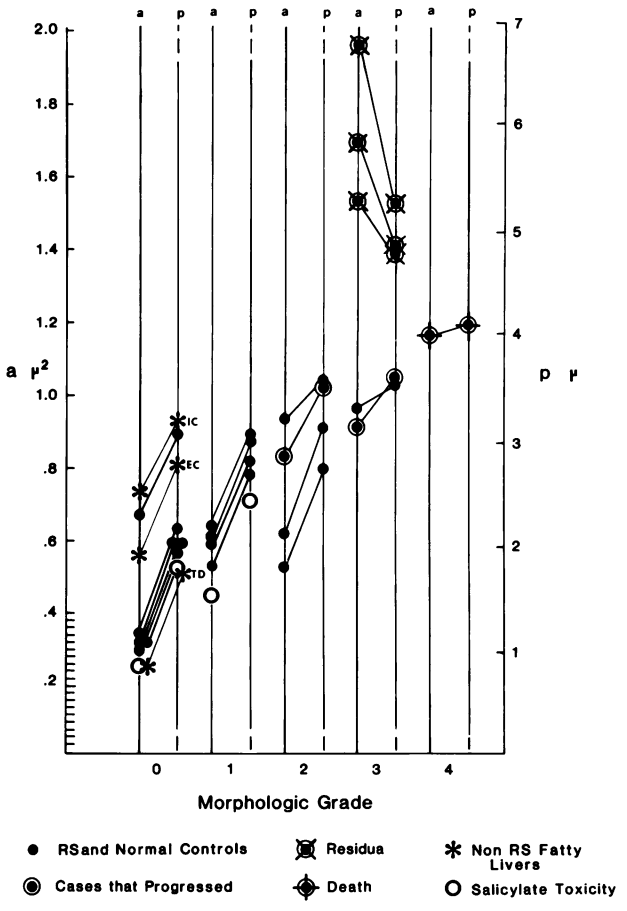

Figure 4—Scattergram. Grade versus mitochondrial area (a) and perimeter (p). Area: $r = 0.8157$, $P = 0.0001$. Perimeter: $r = 0.8632$, $P = 0.0001$. Note the disproportionate size increase in the three cases identified with neurologic residua and the one fatality.

Comparison Between RS and Recovery Liver by Lobular Region (Table 2)

By light microscopy a slight lobular gradient can be observed in fat accumulation (larger periportal droplets) and enzyme depletion (slight periportal retention) in all but the most severe cases. Therefore, a measurable ultrastructural gradient reflecting periportal sparing might be expected. The measured differences, when significant on panlobular comparison, are significant, however, in all lobular regions, including the periportal zone. Significant differences between centrilobular and midzonal, centrilobular and periportal, and midzonal and periportal regions are demonstrable in many parameters in both the RS and recovery samples (not illustrated). Contradictory changes, ie, an increase in one zone balanced by a decrease in another, result in the lack of statistically significant differences between many of these parameters of the RS versus the recovery control liver when the lobule is analyzed as a whole.

Multivariant Analysis (Table 3)

No biasing correlations with sex, prodromal illness, or reason for control biopsy are apparent (not illustrated). Age correlates only with volume density of residual bodies (RBVV, $P = 0.0014$). Lipid volume density (LVV) is highly variable from case to case, showing statistically significant correlation only with serum ammonia ($P = 0.0290$) and stage (initial stage,

Table 2—RS Recovery Comparison by Lobular Region

	Centrilobular		Midzonal		Periportal		Panlobular	
	RS	REC	RS	REC	RS	REC	RS	REC
Hepatocellular								
HA μ^2	499.6	282.6–	297.5	296.3–	432.7	297.3–	381.8	294.3–
LVV	0.243	0.025*	0.273	0.022*	0.236	0.011*	0.256	0.020*
NVV	0.058	0.071*	0.078	0.068*	0.056	0.052*	0.067	0.066–
Na μ^2	20.70	18.44–	20.22	15.64–	23.36	21.85–	20.81	17.11
NoVV	0.0026	0.0041*	0.0030	0.0020*	0.0037	0.0040*	0.0030	0.0027–
Noa μ^2	1.850	2.029–	1.771	1.128*	1.840	1.750–	1.806	1.424–
PVV	0.024	0.013*	0.018	0.011*	0.018	0.013*	0.020	0.012*
Pa μ^2	0.231	0.216*	0.210	0.197*	0.249	0.208*	0.225	0.202*
RBVV	0.0100	0.0170*	0.0063	0.0129*	0.0049	0.0102*	0.0072	0.0130*
RBa μ^2	0.258	0.199*	0.135	0.179*	0.145	0.143*	0.176	0.177–
Mitochondrial								
a μ^2	0.660	0.322	0.542	0.297	0.598	0.312	0.593	0.303*
p μ	3.276	2.129	2.992	2.025	3.133	2.069	3.115	2.049*
NV μ^{-3}	0.172	0.596	0.172	0.742	0.164	0.554	0.171	0.687*
VV	0.103	0.135	0.076	0.141	0.083	0.116	0.086	0.136*
SV μ^{-2}	0.656	1.140	0.523	1.274	0.559	0.966	0.572	1.200*

–, difference not statistically significant ($P > .1100$).

*Statistically significant difference ($P < 0.0081$).

Mean values and significance levels of comparisons between Reye's syndrome and recovery liver. Abbreviations are defined in Table 1 or Figure 2. The last column was generated directly from the pooled data and thus represents a weighted average of the values in the previous three.

Table 3—Multivariant Analysis

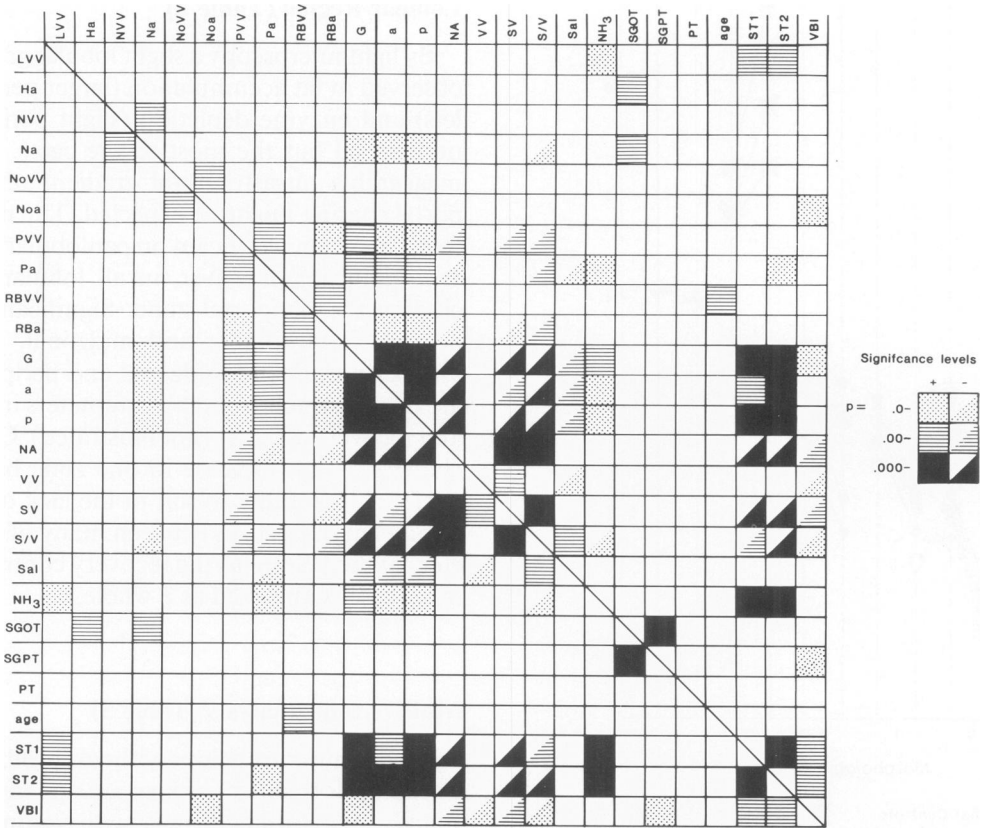

Significance levels of straight line correlations between the multiple analyzed parameters. Abbreviations except for the following are defined in Table 1 or Figure 2: ST1, initial stage; ST2, peak stage.

$P = 0.0024$; peak stage, $P = 0.0094$). Hepatocyte size (Ha) is a complex parameter, reflecting changes in multiple organelle compartments (nucleus, mitochondria, endoplasmic reticulin, etc) as well as osmotic or other forms of cell sap expansion. Ha correlates only with SGOT ($P = 0.0015$). The mean area of peroxisomes (Pa) shows a positive correlation with peroxisomal volume density (PVV, $P = 0.0016$), indicating that size increase accounts for at least a portion of the expansion of the peroxisomal compartment. Only 4 cases show peroxisomal numbers per area above the control range. These include Stages 1–4, Grades 1–2, and none with residual central nervous system (CNS) damage. There is no correlation between peroxisomal numbers and salicylate levels. Both PVV and Pa correlate with morphologic grade ($P = 0.0035$ and 0.0047, respectively), mitochondrial mean area ($P = 0.0224$ and 0.0091) and perimeter ($P = 0.0173$ and 0.0059). Residual bodies as a compartment (RBVV) do not show any disease-related trends. The mean area of individual residual bodies (RBa) correlates, on the other hand, with five of the seven mitochondrial parameters indicating increasing residual body size with increasing lesion severity.

The subjectively determined grade of morphologic severity reflects a visual synthesis of multiple features, mostly related to mitochondrial alteration, but also reflecting changes in other organelle systems. The grade correlates with five of the six mitochondrial parameters ($P = 0.0001$), peroxisomal parameters (PVV, $P = 0.0035$; Pa, $P = 0.0047$), as well as with ammonia ($P = 0.0033$) and initial and peak stage ($P = 0.0001$). This high correlation indicates that the features measured accurately reflect the features visually evaluated in determining the grade.

Enlargement of individual RS mitochondria, as measured by larger area (a) and perimeter (p), correlates strongly with other measures of disease severity (grade, stage). The strikingly reduced numbers of

mitochondria (NA) in the more severe lesions is reflected in reduced surface density (SV) and correlates negatively (as denoted by the minus sign prior to the P value) with initial and peak stage ($P = -0.0001$), vomiting biopsy interval (VBI, $P = -0.0010$), and the peroxisomal values (PVV, $P = -0.0095$, Pa, $P = -0.0485$). Mitochondrial numbers are not reflective of salicylate levels, ammonia, transaminases, or prothrombin time. Ruling out a dilutional effect from hepatocyte swelling, numbers per nucleus are correspondingly reduced, with an identical range of correlations (not shown). NV (number per unit test volume) was also calculated by the Videoplan and other methods indicated in the methods section. All show an identical but less significant range of correlations (not shown).

Some of the mitochondrial correlations are due to mathematical relationships: ie, as area increases, perimeter increases. The negative correlation of grade and stage with number and surface density indicates that as size increases, the number (NA) and amount of surface membrane (SV) decrease. Specific surface (S/V) decrease of individual mitochondria is expected in a population of spheres of increasing size and decreasing number. But S/V also reflects changing irregularity of shape, because the surface proportional to volume of any shape increases with increasing deviation from a sphere.[19] Increasing irregularity of mitochondrial shape would tend, therefore, to mitigate the effects of increased size on S/V.

Because mitochondrial shape alteration is an important feature of RS, quantitation of shape change was also considered. Videoplan-generated non-size-dependent "form factors" based on the ratio of the actual area of a profile to the area of a perfect circle or ellipse calculated from the perimeter of that profile did not adequately reflect the visualized shape change of RS mitochondria, probably because of the averaging influence of increased numbers of tangential and corner profiles as the organelle size and irregularity increase. Lack of reproduceability of form factors with Zeiss equipment has also been attributed to a faulty algorithm.[28]

Although reduced numbers should be reflected in reduced volume density, VV surprisingly correlates with none of the mitochondrial parameters except surface density (SV) and weakly ($P = -0.0499$) with salicylate levels and interval between onset of vomiting and biopsy (VBI, $P = -0.0444$). The volume density of an organelle compartment is determined by the areas of individual organelles as well as their numbers. Analysis of the scattergram (Figure 3) shows a progressive decrease in mitochondrial number (NA) as grade increases. Figure 4 illustrates a disproportionate enlargement of mitochondrial area (a) and perimeter (p) in the 3 morphologic Grade 3 cases which also show increased mitochondrial volume density (VV). These changes cannot be explained by generalized osmotic cell swelling because there is no parallel increase in mean hepatocyte area (Ha), although weak correlations with mean nuclear area (Na), peroxisomal volume proportion (PVV), and mean area (Pa) were noted.

Correlations of morphologic parameters with clinical aspects of the disease other than stage are weak. Serum ammonia correlates with peroxisomal area (Pa, $P = 0.0294$), grade (G, $P = 0.0033$), mitochondrial area (a, $P = 0.0283$), perimeter (p, $P = 0.0168$), specific surface (S/V, $P = 0.0410$), and initial and peak stage (ST1 and ST2, $P = 0.0001$). SGOT correlates with hepatocyte area (Ha, $P = 0.0015$), nuclear area (Na, $P = 0.0065$) and SGPT ($P = 0.0001$). SGPT correlates strongly only with SGOT. Prothrombin time shows no significant correlations.

Salicylate levels show a negative correlation with grade of mitochondrial severity (G, $P = -0.0044$) as well as area (a) and perimeter (p). No correlation of serum salicylate with clinical stage is identified. This is not due to increasing time after last dose since the probability of correlation with VBI is very low ($P = -0.2690$).

The interval of time between onset of vomiting until biopsy (VBI) was investigated as the best measure of the time between disease onset and biopsy. A weak association with nucleolar area (Noa), possibly reflecting increased DNA and RNA replication as recovery begins, was noted. VBI also correlates weakly with mitochondrial grade ($P = 0.0129$) and number (NA, $P = -0.0010$), showing a tendency for the lesion to be worse in later cases. Because VBI also correlates with initial ($P = 0.0047$) and peak stage ($P = 0.0098$), children biopsied later in their disease may be more likely to have a severe lesion.

Although not all children with a severe lesion have severe clinical disease, higher morphologic grade, lower mitochondrial numbers, larger mitochondrial areas and longer perimeters are strongly associated with higher clinical stage and progression (Table 1 and Figures 3 and 4). Six of the 14 cases progressed to a higher clinical stage after admission. Of these, 5 required a craniotomy for monitoring of intracranial pressure (ICP), and 1 case a decompressive craniectomy as well. Two patients recovered completely, 1 died, and 3 were left with mild neurologic residua (Table 1). None of the nonprogressive cases experienced similar difficulties. The 3 cases with neurologic residua and the 1 fatal case show the greatest reduction in mitochondrial number and are clearly identi-

fied by an increased mitochondrial a and p (Figures 3 and 4).

Disease Controls

One (patient SB) of the two salicylate toxicity cases included in an attempt to identify a factor independently related to salicylate levels overlaps in terms of mitochondrial numbers (NA), area (a), and perimeter (p) with the mild RS cases. This overlapping child had been vomiting for 76 hours prior to biopsy and presented with lethargy, confusion, and combativeness rapidly progressing to decerebrate posturing and anisocoria. These symptoms could be considered consistent with clinical Stage III RS. There is, however, no excessive hepatic lipid; and succinic acid dehydrogenase activity is normal. An earlier peak salicylate level of 66 mg/dl with minor quantitative and qualitative hepatic morphologic changes (evaluated as equivalent to the Grade 1 alteration of RS), but severe neurologic symptoms are more consistent with salicylate toxicity than RS.

The non-RS fatty liver controls are quantitatively unlike the RS livers (Figures 3 and 4). The autopsy case (patient IC) shows typical shock induced mitochondrial enlargement (a and p, Figure 4) with matrix hypolucency, loss of matrix granules, and matrix densities. The slightly reduced mitochondrial number (NA, Figure 3), not overlapping with RS, probably reflects dilutional effects of osmotic hepatocellular swelling. The child with carnitine deficiency (patient EC) shows control numbers (NA, Figure 3) of slightly larger (a and p, Figure 4) but otherwise normal-appearing mitochondria. The liver of the child on therapy for dermatomyositis (patient TD), except for the lipid, is identical to nonfatty morphologically normal livers.

Ultrastructural Histochemistry

Mitochondria are labeled with dark black formazan pigment precipitate, indicating preserved cytochrome oxidase activity in a pattern consistent with inner membrane localization (Figure 5). The staining related to individual mitochondria in RS is no different than the PKU and recovery control.

Discussion

The mitochondrial enlargement in RS, readily apparent in typical micrographs, is confirmed by a mea-

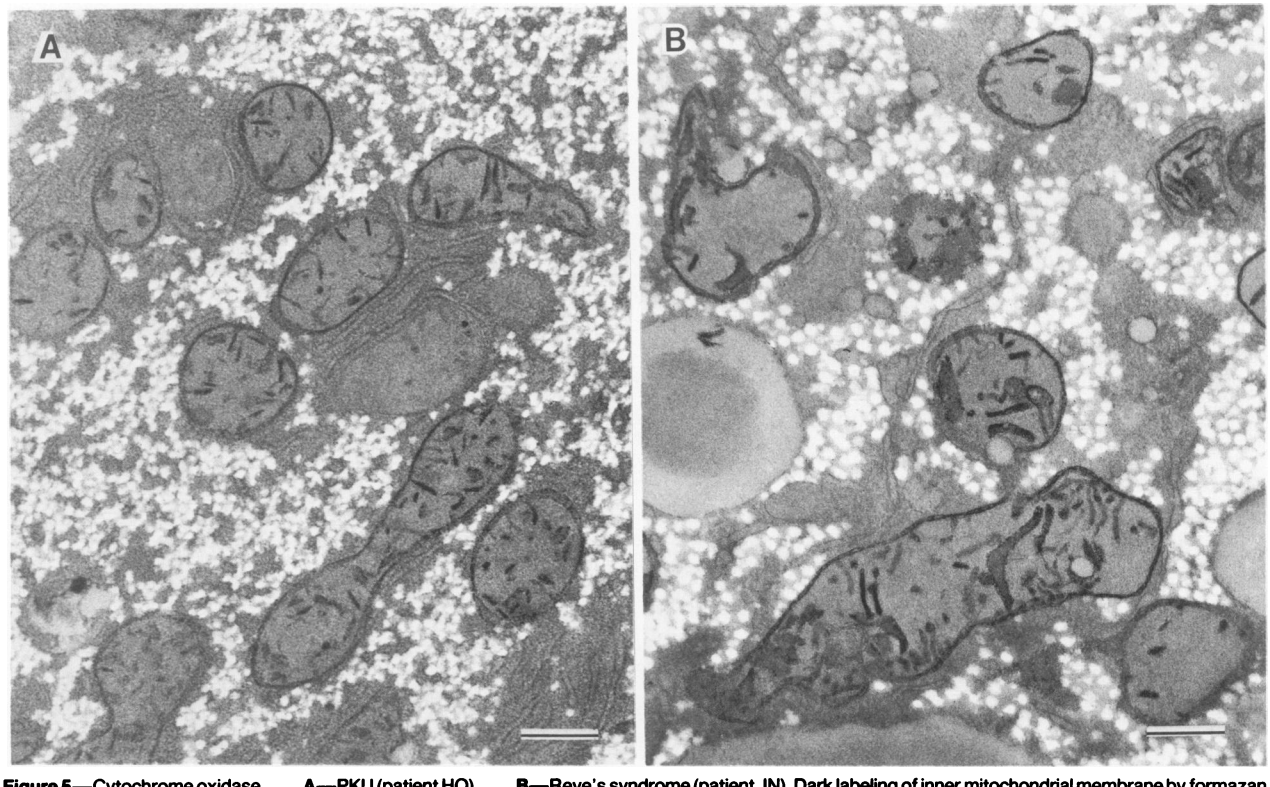

Figure 5—Cytochrome oxidase. **A**—PKU (patient HO). **B**—Reye's syndrome (patient JN). Dark labeling of inner mitochondrial membrane by formazan reaction product indicating preserved enzyme activity in both PKU control and RS. Bar = 0.5 μ.

surable increase in area (a) and perimeter (p). Less apparent, unless equally magnified areas are compared, is the decreased mitochondrial number (NA). This decrease is reflected in decreased volume and surface density (VV, SV). Size parameters correlate positively, and numerical density negatively, with clinical stage.

Decreased mitochondrial numbers have not previously been emphasized and seem based on these results, to be specific for RS, implying a basic biologic mechanism resulting in a global deficit of mitochondrial function. This finding certainly reflects an aspect of the disease biology not previously considered, providing a link to the understanding of light-microscopic enzyme histochemical preparations, because fewer mitochondria can result in reduced staining intensity for mitochondrial enzymes as well as nonfunctional mitochondria. The retained cytochrome oxidase staining in individual RS mitochondria at the ultrastructural level supports this concept (Figure 5). Volume density and surface density should correlate best with biochemical quantitation[5] and in RS must reflect the decreasing number of mitochondria. A decreased proportion of the mitochondrial isoenzyme of SGOT (aspartate aminotransferase) in the serum[29] is also interpretable as a result of reduced numbers of hepatic mitochondria. Correlations with biochemical assays of enzyme activity in liver would further increase understanding of the process.

One clue to the fate of the vanished mitochondria is the more frequent fragmented profiles in severe lesions. None are seen in autophagic vacuoles. Fusion as another possible mechanism for number reduction (and size increase as well) is suggested by profiles of adjacent mitochondria with apparent breakdown of intervening membranes (Figure 1D and 6B). It seems likely that remaining mitochondria retain some functional capacity; necrosis in RS livers is the exception, rather than the rule; and as shown by the two recovery biopsies, RS livers return to normal very quickly with no apparent residua. Hepatocytes with "diagnostic" RS mitochondria often appear otherwise relatively healthy, with cytoplasmic glycogen, lamellar profiles of rough endoplasmic reticulum wrapped around RS mitochondria, nondilated nuclear cisternae with a normal nuclear chromatin pattern (Figures 1 and 6A)

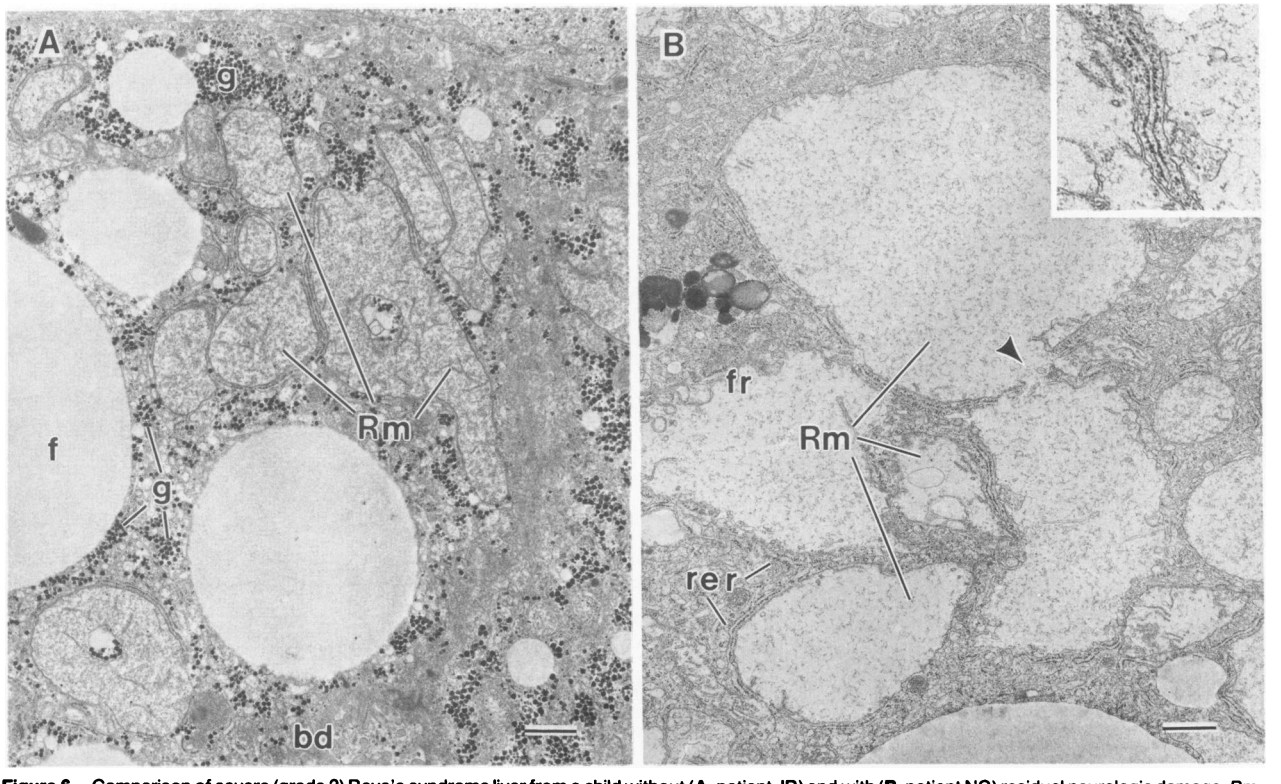

Figure 6—Comparison of severe (grade 3) Reye's syndrome liver from a child without (**A**, patient JB) and with (**B**, patient NC) residual neurologic damage. *Rm*, RS mitochondria; *rer*, intact rough endoplasmic reticulum; *fr*, membrane fragmentation; *g*, glycogen. *Arrow* indicates fragmentation of apposed membranes with fusion of profiles. **Inset** from center of **B**—Relatively intact rough endoplasmic reticulum wrapped around a severely affected RS mitochondrion. Bar = 1 μ. **inset** magnified an additional two times.

and can occasionally be seen in mitosis. Ultrastructural retention of cytochrome oxidase activity (Figure 5), while not representing all enzymes, is an additional clue that metabolic capacity is retained in remaining mitochondria.

It is known that mitochondria fuse and divide, but processes responsible for mitochondrial replication, growth, and turnover are poorly understood.[30,31] Relative roles of nuclear and mitochondrial DNA, sites of manufacture of some mitochondrial proteins, and methods of transport into mitochondria are just now being delineated.[32] The insult responsible for RS is perhaps toxic to mechanisms for maintaining steady state numbers, rather than directly to mitochondrial function. Further understanding of these findings is not possible until more is known about the biogenesis, senescence, and steady state maintenance of mitochondria.

Decreased numbers were not addressed in recent nonquantitative analysis of RS hepatic mitochondrial grade.[15] Morphometric analysis of an animal model has to our knowledge only once been done,[33] and illustrations in other models concentrate only on a few altered mitochondria with no quantitative information.[34] Such knowledge would greatly enhance understanding of the relationship of various animal models to human disease.

While reduced mitochondrial numbers are of significance, massive increase in size more clearly identifies the 3 cases with neurologic damage severe enough to result in residual dysfunction. The possibility that this disproportionate area increase is due to generalized osmotic cell swelling, signaling generalized decompensation of membrane osmotic integrity, is unlikely, because there is no parallel disproportionate increase in the cross-sectional area of hepatocytes (Ha). The mitochondrial morphology of a Grade 3 case without neurologic residua (patient JB), compared with a Grade 3 case, with residua (patient NC) is suggestive of massive mitochondrial matrix expansion and increased membrane fragmentation (Figure 6), perhaps a sign of end-stage mitochondrial decompensation. The link between this and central nervous system damage remains unclear.

Mitochondria are not the only organelles altered in RS. However, unless a cell is frankly moribund, other organelles remain relatively intact. Ribosomes remain attached to endoplasmic reticulum until the end-stages of degeneration, and alpha-glycogen is often present, particularly in modern cases when glucose has been administered (Figures 1D and 6). Changes such as vesiculation of endoplasmic reticulum and ribosomal disaggregation are thus probably secondary to generalized, late hepatocellular degeneration. The proliferation of smooth endoplasmic reticulum sometimes observed may be related to glycogen or drug metabolism. Quantitative changes in endoplasmic reticulum were not addressed in this study. Peroxisomes often show swelling and flocculation with increased volume percent and mean area. The qualitative alteration is not distinctive and can be seen in diverse situations. Statistically significant associations of peroxisomal values are not as strong as those of mitochondria, particularly to clinical parameters. Scattergrams do not show any association of peroxisomal values to individual cases with high salicylate levels or poor prognosis. Because of their role in peroxidative detoxification and lipid metabolism, peroxisomes are likely to have an important role, but these data suggest secondary involvement.

Intralobular variation in lesion severity is a feature of many cases of RS, with more severe lesions showing more uniform alteration. Periportal sparing of histochemical enzyme activity is visible by light microscopy in milder but less apparent in more severe cases. Significant statistical differences in many measured parameters of one Grade 2 case (patient RB), between lobular regions of both the illness and follow-up biopsy, reflect an irregular mosaic-like intralobular variation in severity. A balanced panlobular representation was, therefore, required as the most accurate reflection of average hepatic functional capacity. When significant differences between RS and non-RS parameters generated from the entire lobule do occur, they reach statistical significance independently in all three lobular zones, contradicting the notion of periportal sparing suggested by the preservation of histochemically detectable enzyme activity. Therefore, studies on limited material may be valid in a diagnostic, if not quantitative, sense.

Two cases of salicylate toxicity were included in the multivariant analysis, attempting to identify features independently associated with salicylism. Each is either identical, or nearly so, to controls. Salicylate levels show negative correlation with lesion severity (grade, mitochondrial area and perimeter) and no correlation with stage, despite the epidemiologic association of RS with salicylate administration.[35] If salicylates do not directly cause RS, but act synergistically by uncoupling oxidative phosphorylization, lower salicylate dosage may be sufficient to cause more severe clinical disease in children more severely affected by RS. No correlations of salicylate levels with morphometric parameters independent of RS disease-related parameters were discovered.

The three non-RS fatty livers do not show other features of RS. Although the common nonspecific autopsy finding of hepatic lipid accumulation[12]

makes RS difficult to prove by autopsy criteria alone, the fatty liver from the autopsied child was quantitatively distinct from RS, showing shock-enlarged mitochondria (Figure 4) without number reduction (Figure 3). This indicates that shock and autolysis alone probably do not result in decreased mitochondrial numbers. Within the context of this series, mitochondrial number reduction is characteristic of RS and may provide a criterion helpful in the assessment of postmortem livers in which the diagnosis of RS is equivocal.

This retrospective study sought to define the quantifiable aspects of the RS hepatic lesion which relate to pathophysiology and diagnostic specificity. Although these data cannot appropriately address the question of predicting clinical deterioration, massive mitochondrial enlargement superimposed on severe number reduction clearly identified the 3 cases in this series with CNS damage severe enough to result in residual neurologic malfunction after hepatic recovery. Reduction in mitochondrial numbers alone, above a threshold necessary for viability, may not always accurately reflect the actual clinical severity and progression of RS, if a second mitochondrial insult is necessary for the manifestation of clinical symptoms. Thus, not only salicylates, but any insult further impairing the function of reduced numbers of mitochondria (ie, hypoglycemia, dehydration-induced shock, other mitochondrial toxins such as insecticides or salicylates) might synergistically tip the patient toward clinically manifest RS and progression. Our data are supportive; but a large, ideally prospective, study would be needed to confirm this hypothesis.

References

1. Reye RDK, Morgan G, Baral J: Encephalopathy and fatty infiltration of the viscera: A disease entity in childhood. Lancet 1963, 2:749–752
2. Devivo DC: Reye syndrome: A metabolic response to an acute mitochondrial insult. Neurology 1978, 28:105–108
3. Partin JC, Schubert WK, Partin JC, Partin JS: Mitochondrial ultrastructure in Reye's Syndrome (encephalopathy and fatty degeneration of the viscera). N Engl J Med 1971, 285:1339–1343
4. Bove KE, McAdams AJ, Partin JC, Partin JS, Hug G, Schubert WK: The hepatic lesion in Reye's syndrome. Gastroenterology 1975, 69:685–697
5. Mitchell RA, Ram ML, Arcinue EL, Chang CH: Comparison of cytosolic and mitochondrial enzyme alterations in Reye's Syndrome. Pediatr Res 1980, 14:1216–1221
6. Aprille JR: Abnormal mitochondria and the search for causative agents in Reye's syndrome, Reye's Syndrome IV, Edited by JD Pollack. Bryan, Ohio, National Reye's Syndrome Foundation 1985, pp 153–162
7. Partin JS, McAdams AJ, Partin JC, Schubert WK, McLaurin RL: Brain ultrastructure in Reye's Disease: II. Acute injury and recovery processes in three children. Neuropathol Exp Neurol 1978, 37:796–819
8. Robinson BH, Taylor J, Cutz E, et al: Reye's syndrome: Preservation of mitochondrial enzymes in brain and muscle compared with liver. Pediatr Res 1978, 12:1045–1047
9. Mitchell RA, Partin JC, Partin JS, et al: Hepatic and encephalopathic components of Reye's syndrome: Factor analysis of admission data from 209 patients. Neurology 1985, 35:1236–1239
10. Svobada DJ, Reddy JK: Pathology of the liver in Reye's syndrome. Lab Invest 1975, 32:571–579
11. Starko KM, Mullick FG: Hepatic and cerebral pathology findings in children with fatal salicylate intoxication: further evidence for a causal relationship between salicylate toxicity and Reye's Syndrome. Lancet 1982, 11:326–329
12. Bonnell HJ, Beckwith JB: Fatty liver in sudden childhood death. Am J Dis Child 1986, 140:30–33
13. Daugherty CC: Liver morphology in clinically staged Reye's syndrome. Lab Invest 1982, 46:4p
14. Lichtenstein PK, Heubi JE, Daugherty CC, Farrell MK, Sokol RJ, Rothbaum RJ, Suchy FJ, Balistreri WF: Grade I Reye's syndrome, a frequent cause of vomiting and liver dysfunction after varicella and upper respiratory tract infection. N Engl J Med 1983, 309:133–139
15. Chang CH, Uchwat F, Masalskis R, Arcinue EL: Morphologic grading of hepatic mitochondrial alteration in Reye's syndrome: Potential prognostic implication. Pediatr Pathol 1985, 4:265–275
16. Partin JS, Daugherty CC, McAdams AJ, Partin JC, Schubert WK: A comparison of liver ultrastructure in salicylate intoxication and Reye's syndrome. Hepatology 1984, 4:687–690
17. Schubert WK, Partin JC, Partin JS: Encephalopathy and fatty liver (Reye's syndrome). Prog Liver Dis 1972, 4:489–510
18. Peachey LD: Quantitative analysis of electron micrographs, short course, Marine Biological Laboratory, Woods Hole, Massachusetts, December 7–12, 1980
19. Williams MA: Quantitative Methods in Biology: Practical Methods in Electron Microscopy. Vol 6. New York, Edited by AM Glaucert. North Holland, 1976
20. Aherne WA, Dunnill MS: Morphometry. London, Edward Arnold, 1982
21. Rohr H, Oberholzer M, Bartscha G, Keller M: Morphometry in experimental pathology, methods, baseline data, applications, International Review of Experimental Pathology. Edited by GW Richter, MA Epstein. New York, Academic Press, 1976, pp233–322
22. Loud A: A quantitative stereological description of the ultrastructure of normal rat liver parenchymal cells. J Cell Biol 1968, 37:27–46
23. Ma MG, Biempca L: The normal human liver cell. Am J Pathol 1971, 62:353–375
24. Videoplan Operating Manual, 1981, 1984 Update, Carl Zeiss, Inc.
25. Underwood EE: Quantitative Stereology. Reading, Addison-Wesley, 1970
26. Hanker JS: Oxidoreductases, The Electron Microscopy of Enzymes. Vol 4. Edited by MA Hayat. New York, Van Nostrand Reinhold 1975, pp1–125
27. True LD, Nakane PK: Immunoelectromicroscopy, Current Trends in Morphological Techniques. Vol 3. Edited by JE Johnson. Boca Raton, CRC Press, 1981, p 104
28. Pitha JU: Computer assisted planimetry. Hum Pathol 1985, 16:1284–1285
29. Mock DM, Scott M, Mock NI, Thaler MM: The proportion of mitochondrial isoenzyme of aspartate aminotransferase is not elevated in Reye's syndrome. Pediatr Res 1983, 17:884–888

30. Brachet J: Semiautonomous cell organelles, Molecular Cytology. Orlando, Academic Press, 1985, pp 121–169
31. Lee CP, Schnatz G, Dallner G, eds. Mitochondria and Microsomes. Reading, Addison-Wesley, 1981
32. Parikh VS, Morgan MM, Scott R, Clements LS, Butow RA: The mitochondrial genotype can influence nuclear gene expression in yeast. Science 1987, 235:576–580
33. Gray RH, Deshmukh DR, Maassab JF, Robertson DG, de la Iglesia FA, edited by GW Bailey: Structural and morphometric studies of liver in a ferret model of Reye's syndrome, Proceedings of the 41st Annual Meeting of the Electron Microscopy Society of America. San Francisco, San Francisco Press, 1983, pp 806–807
34. Deshmukh DR: Animal models of Reye's Syndrome. Rev Infect Dis 1985, 7:31–40
35. National Surveillance for Reye Syndrome 1981: Update, Reye Syndrome and salicylate usage. MMWR 1982, 31:53–61

Acknowledgments

I would like to thank Dr. A. J. McAdams for helping to make my writing understandable, Dr. J. and J. Partin for their patience and generous sharing of valuable cases and many of the basic concepts developed in this project, K. Field for her typing of multiple revisions of this manuscript, and Cherie Kessler for making the publication prints on her day off.